GEORG-AUGUST-UNIVERSITÄT
GÖTTINGEN

Fakultät für
Physik

Bachelors Thesis

Skalentheorie für die Tropfengrößenverteilung in Niederschlägen

Scaling Theory for the Droplet Size Distribution of Precipitation

prepared by

Ariane Papke

from Delmenhorst

at the Max Planck Institute for Dynamics and Self-Organization

Thesis period: 8th April 2011 until 15th July 2011

First referee: Prof. Dr. Jürgen Vollmer

Second referee: Prof. Dr. Karl-Henning Rehren

Contents

1. Motivation

A multitude of physical processes contribute to the formation and growth of rain droplets [6]. Among these, we will be particularly interested in the nucleation and formation of rain droplets by collision and coalescence in a supersaturated environment [8, 9]. The driving processes are the temperature change and the turbulent mixing of water vapor, resulting in moisture. When droplets reach a certain size they start feeling gravity and leave the cloud as rain. In a specially designed lab experiment this precipitation removes the moisture, and the rain formation starts all over [4, 10]. In recent experiments it became possible to measure the evolution of the size distribution of the droplets in the course of this process [4].

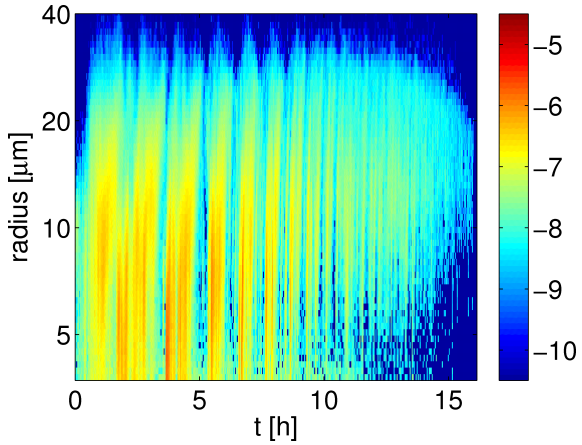

Figure 1.1.: Measured distribution of droplet sizes as a function of time. Colours indicate the density of particles in the lower layer on a logarithmic scale. The turbidity varies periodically (with a decreasing period), and when the turbidity is high there is a wide range of droplet sizes. Figure reproduced from [7].

A long-standing question in modeling this feature is in how far Ostwald ripening [3] plays a role in its evolution. Assuming the supersaturation in a system is low and initiated by a quench experiment and afterwards kept at a constant temperature, the birth of new droplets is insignificant. In Lifshitz-Slyozov-theory (LS-theory) the

diffusive process in a solid solution of spherical droplets without elastic stresses is surveyed [5]. With means of classical nucleation theory they derived a differential equation for the growth of droplets in a system and proved that the associated droplet size distribution assumes a time-invariant scaling form. One of the objectives of this thesis will be to explore in how far this model must be revised due to the fact that the temperature, and hence also the ambient supersaturation, is constantly changing in clouds.

Following LS-theory we will adopt a scaling ansatz for the droplet size distribution. We will work out a model that reproduces the scaling distribution and can be adapted to different processes in a cloud. Applying a constant heating rate lets us review the processes in a cloud without paying attention to the spatial temperature differences. Then, if the droplets are big enough and fall due to gravitation through the cloud, they sweep up smaller droplets that will not form new rain droplets but leave the system.

2. Theory

2.1. Growth of Individual Droplets

In this section we revisit basics on the growth of individual droplets in a supersaturated steam, as presented by Landau and Lifshitz [3].

Given a metastable state, i.e., a supersaturated solution, liquid droplets form due to fluctuations. Then the drops need to compensate inter-phase surface tension and there is a critical size a_c where they neither shrink nor grow. Droplets that have a radius $a > a_c$ are stable and persist. We consider the growth of macroscopic droplets, i.e. metastable states far away from phase instabilities, assuming them to be spherical.
The critical droplet size a_c can be determined by maximizing the change in free energy. It depends on the surface tension α, the difference of the chemical potentials $\Delta\mu$ of the two phases and the volume per droplet v'. Given the free energy per volume Δf, the radius a of a droplet and its surface A_d, the change in free energy with respect to the spatially uniform state is

$$\Delta F(a) = -v'\Delta f + A_d\alpha = -\frac{4\pi}{3}a^3\Delta f + 4\pi a^2\alpha.$$

Assuming that the droplet is big enough to consider the surface and volume to be described by thermodynamic bulk quantities, Δf and α do not depend on a. Hence, the critical radius $a_c \neq 0$ that arises at a maximum of ΔF is

$$a_c = \frac{2\alpha}{\Delta f} \quad \Leftrightarrow \quad 0 = -4\pi a_c^2\Delta f + 8\pi a_c\alpha.$$

Moreover, with N the number and V_{tot} the volume of all droplets, due to the Gibbs relation $\mathrm{d}f = \mathrm{d}\frac{F}{V_{\text{tot}}} = \frac{N}{V_{\text{tot}}}\mathrm{d}\mu$ the free energy difference per unit volume amounts to

$\Delta f = \dfrac{\Delta\mu}{v'}$. So we find an expression for the critical radius:

$$a_c = \frac{2\alpha v'}{\Delta\mu}.$$

Let c be the mean concentration of the solution, $c_{0\infty}$ the concentration of the saturated solution on a plane surface, $\Delta := c - c_{0\infty}$ and T the temperature. Then for a diluted solution we can express the chemical potential difference as

$$\Delta\mu = T \ln \frac{c}{c_{0\infty}} \approx \frac{T(c - c_{0\infty})}{c_{0\infty}} = \frac{T\Delta}{c_{0\infty}}$$

This leads to a critical radius

$$a_c = \frac{2\alpha v' c_{0\infty}}{T\Delta} \tag{2.1}$$

and determines the equilibrium concentration c_{0a} at the surface of a droplet

$$c_{0a} = c_{0\infty} + \frac{a_c}{a}\Delta. \tag{2.2}$$

Introducing the variable $\sigma := 2\alpha v' c_{0\infty}/T$ and inserting (2.1) into (2.2) we find

$$c_{0a} = c_{0\infty}\left(1 + \frac{2\alpha v'}{Ta}\right) = c_{0\infty} + \frac{\sigma}{a}.$$

Since drops grow due to diffusion, the concentration change by growing or shrinking droplets is described by the diffusion equation. Assuming that the concentration quasistatically adapts to the droplet size we find a stationary solution $c(r)$ to the diffusion equation in spherical coordinates,

$$D\frac{1}{r}\frac{\partial^2}{\partial r^2} r c(r) = \frac{\partial c(r)}{\partial t} = 0 \Rightarrow c(r) = c - (c - c_{0a})\frac{a}{r}$$

where D is the diffusion coefficient and t the time. The concentration change drives a diffusive current

$$\dot{a} = -j(a) = D\left.\frac{\partial c}{\partial r}\right|_{r=a} = \frac{D}{a}\left(\Delta - \frac{\sigma}{a}\right) = \frac{D\sigma}{a^2}\left(\frac{a\Delta}{\sigma} - 1\right).$$

According to previous explanations the critical radius is determined by $j(a_c) = 0$ such that $a_c(t) = \sigma/\Delta(t)$.

Now we will consider a system of N droplets with radii a_i, $i = 1, \ldots, N$. Measuring time in units of $a_c^3(0)/D\sigma$ and the radius in units of $a_c(0) := 1$ we get for every droplet i the equation

$$\dot{a}_i = \frac{1}{a_i^2}\left(\frac{a_i}{a_c} - 1\right). \tag{2.3}$$

Consequently, for a quench experiment where the overall droplet volume[1] V_{tot} is fixed by the Maxwell phase rule [2] the critical radius a_c amounts to the mean droplet radius $\overline{a} := N^{-1}\sum_i a_i$:

$$V_{\text{tot}} = \sum_i a_i^3 = \text{const.} \Rightarrow 0 = \sum_i a_i^2 \dot{a}_i = \frac{\sum_i a_i}{a_c} - N = N\left(\frac{\overline{a}}{a_c} - 1\right) \Rightarrow \overline{a} = a_c.$$

In the experiment of Lapp et al.[2] a constant heating rate is applied which is chosen such that the volume changes linearly in time. To account for the change of T we adapt equation (2.3) to take the form

$$\dot{a}_i = \frac{1}{a_i^2}\left(\frac{a_i}{\overline{a}} - k\right) \quad \text{where } k \in \mathbb{R}. \tag{2.4}$$

Consequently, the parameter k describes an increasing volume for $k < 1$ and a decreasing volume for $k > 1$. After all,

$$\dot{V}_{\text{tot}} = \sum_{i=1}^{N} \frac{\mathrm{d}a_i^3}{\mathrm{d}t} = 3\sum_{i=1}^{N} a_i^2 \dot{a}_i = 3\sum_{i=1}^{N}\left(\frac{a_i}{\overline{a}} - k\right) = 3N(1-k) \tag{2.5a}$$

$$\text{if } N = \text{const.} \Rightarrow V_{\text{tot}} = V_0 + 3N(1-k)\,t \quad \text{where } V_0 = V(0) = \text{const.} \tag{2.5b}$$

2.2. Scaling Theory for the Droplet Size Distribution

2.2.1. Deriving the Size Distribution

In order to work out an expression for the droplet size distribution we start from a scaling ansatz for the droplet density $n(a,t)$ of droplets of radius a per volume at a certain time t. Firstly, the density decreases in time. We assume decay according to

[1] In our considerations we suppress constant coefficients, like $\frac{4}{3}\pi$, because they do not change the physics of the scaling laws which we explore in the present thesis.

[2] T. Lapp, M. Rohloff, J. Vollmer, M. Wilkinson and B. Hof. *Test-tube model for rainfall*, in preparation

a power law so that we can isolate the time dependence. Secondly, we assume that apart from the given time scaling the distribution just depends on the combination of a and t,

$$n(a,t) = t^{-\beta}\hat{n}\left(\frac{a}{t^\alpha}\right), \qquad \text{where } \alpha, \beta \in \mathbb{R}. \tag{2.6}$$

Starting from the density we calculate the total volume V_{tot} of all droplets in the considered system, the number N of droplets, and the average radius $\overline{a}$ of droplets

$$\begin{aligned} V_{\text{tot}} &= \sum_i a_i^3 = \int_0^\infty a^3 n(a)\mathrm{d}a \\ N &= \sum_i = \int_0^\infty n(a)\mathrm{d}a \\ \overline{a} &= \sum_i \frac{a_i}{N} = \frac{1}{N}\int_0^\infty an(a)\mathrm{d}a \end{aligned}$$

Taking into account (2.5a) we write for a constant c_v

$$V_{\text{tot}}(t) = c_v t^\lambda \stackrel{!}{=} t^{4\alpha-\beta} \underbrace{\int_0^\infty \left(\frac{a}{t^\alpha}\right)^3 \hat{n}\left(\frac{a}{t^\alpha}\right) \mathrm{d}\left(\frac{a}{t^\alpha}\right)}_{c_v} \tag{2.7a}$$

$$\Rightarrow \lambda = 4\alpha - \beta \tag{2.7b}$$

where $\lambda = 0$ for a quench experiment and $\lambda = 1$ for constant flux heating. This provides a first relation between the parameters α, β and λ.
In the same way, inserting the ansatz, we rewrite the number of droplets

$$N = t^{\alpha-\beta}\int_0^\infty \hat{n}(x)\,\mathrm{d}x. \tag{2.8}$$

Then we calculate the average radius $\overline{a}$ using above formulas and observe

$$\begin{aligned} \overline{a} &= \frac{t^{2\alpha-\beta}\int_0^\infty \frac{a}{t^\alpha}\,\hat{n}\left(\frac{a}{t^\alpha}\right)\mathrm{d}\left(\frac{a}{t^\alpha}\right)}{t^{\alpha-\beta}\int_0^\infty \hat{n}\left(\frac{a}{t^\alpha}\right)\mathrm{d}\left(\frac{a}{t^\alpha}\right)} \\ &= c_a t^\alpha \end{aligned} \tag{2.9}$$

with a constant c_a.
The average droplet size grows according to a power law with exponent α. We define

$x := \frac{a}{t^\alpha}$, and can hence write

$$\frac{\overline{a}}{t^\alpha} = c_a = \frac{\int x\,\hat{n}(x)\mathrm{d}x}{\int \hat{n}(x)\mathrm{d}x} =: \overline{x}$$

As a final step we check under which conditions the scaling ansatz (2.6) is consistent with the time evolution (2.4). To this end we observe that droplets disappear from the system only by shrinking to zero size. Consequently, $n(a,t)$ evolves according to an advection-diffusion equation with an absorbing boundary condition at $a = 0$.

$$\begin{aligned}
&\dot{n}(a,t) = -\partial_a j_a, \\
\text{where} \qquad &-\partial_a j_a = -\partial_a(\dot{a}n) = -t^{-\beta}\dot{a}t^{-\alpha}\,\hat{n}' - t^{-\beta}\,\hat{n}\left(-\frac{a}{a^3\overline{a}} + \frac{2k}{a^3}\right) \\
&\qquad\qquad = -t^{-\beta-\alpha}\frac{1}{a^2}\left(\frac{a}{\overline{a}} - k\right)\hat{n}' + \frac{t^{-\beta}}{a^3}\left(\frac{a}{\overline{a}} - 2k\right)\hat{n}, \\
\text{and} \qquad &\dot{n}(a,t) \overset{!}{=} -\beta t^{-\beta-1}\hat{n} - \alpha t^{-\beta-\alpha-1} a\,\hat{n}' \quad \text{using (2.6).}
\end{aligned}$$

$$\begin{aligned}
\Leftrightarrow -t^{-\beta-\alpha}\frac{1}{a^2}\left(\frac{a}{\overline{a}} - k\right)\hat{n}' + \frac{t^{-\beta}}{a^3}\left(\frac{a}{\overline{a}} - 2k\right)\hat{n} &= -\alpha t^{-\beta-\alpha-1} a\,\hat{n}' - \beta t^{-\beta-1}\,\hat{n} \\
\Leftrightarrow -\frac{t^{1-\alpha}}{a^2}\left(\frac{a}{\overline{a}} - k\right)\hat{n}' + \frac{t}{a^3}\left(\frac{a}{\overline{a}} - 2k\right)\hat{n} &= -\alpha\frac{a}{t^\alpha}\,\hat{n}' - \beta\,\hat{n} \qquad (2.10)
\end{aligned}$$

Since $\hat{n}$ does not depend on t or a independently, but only via $x = \frac{a}{t^\alpha}$ consistency requires that the coefficients must be functions of x. This requires

$$\frac{t^{1-\alpha}}{a^2} = \left(\frac{t^\alpha}{a}\right)^2 = \frac{1}{x^2}, \qquad \frac{t}{a^3} = \left(\frac{t^\alpha}{a}\right)^3 = \frac{1}{x^3} \qquad \Rightarrow\ \alpha = \frac{1}{3}$$

Without an assumption on λ, i.e. on the volume growth, we find that $\alpha = 1/3$. β is determined by (2.7b) to be $\beta = 4/3$ for the case $\lambda = 0$ (LS-theory) and $\beta = 1/3$ for the case $\lambda = 1$ (constant heating). We examine the latter case and insert these findings and (2.9) into (2.10)

$$\begin{aligned}
\alpha x\,\hat{n}' - \frac{1}{x^2}\left(\frac{a}{\overline{a}} - k\right)\hat{n}' + \frac{1}{x^3}\left(\frac{a}{\overline{a}} - 2k\right)\hat{n} + \beta\,\hat{n} &= 0 \\
\Leftrightarrow \left[\alpha x - \frac{1}{x^2}\left(\frac{x}{c_a} - k\right)\right]\hat{n}' + \left[\frac{1}{x^3}\left(\frac{x}{c_a} - 2k\right) + \beta\right]\hat{n} &= 0
\end{aligned}$$

$$\Leftrightarrow \frac{\mathrm{d}\,\hat{n}}{\mathrm{d}x} = -\frac{\beta x^3 + \dfrac{x}{c_a} - 2k}{\alpha x^3 - \dfrac{x}{c_a} + k}\,\frac{\hat{n}}{x} \tag{2.11}$$

To solve this equation it is worthwhile to get rid of the singularity at $x = 0$ by introducing $f(x) = \dfrac{\hat{n}}{x^2}$. This transforms the differential equation to

$$\begin{aligned}\frac{\mathrm{d}f}{\mathrm{d}x} = \frac{\mathrm{d}\,\hat{n}}{\mathrm{d}x}\,x^{-2} - 2\frac{f}{x} &= \left(\frac{-\beta x^3 - \dfrac{x}{c_a} + 2k}{\alpha x^3 - \dfrac{x}{c_a} + k} - 2\right)\frac{f}{x} \\ &= \frac{-(2\alpha+\beta)x^2 + \dfrac{1}{c_a}}{\alpha x^3 - \dfrac{x}{c_a} + k}\,f \end{aligned} \tag{2.12}$$

According to (2.7b) the expression becomes $2\alpha + \beta = 1$ and the equation is solved by

$$f(x) = \frac{C}{\dfrac{x^3}{3} - \dfrac{x}{c_a} + k}$$

with a constant $C \in \mathbb{R}$. As the distribution is just defined up to a normalization constant, we choose $C = 1$ without loss of generality. To analyze the distribution $\hat{n}$, again we have to transform this solution back using $\hat{n} = x^2\,f(x)$ leading to

$$\hat{n}(x) = \frac{x^2}{\dfrac{x^3}{3} - \dfrac{x}{c_a} + k}. \tag{2.13}$$

It is now difficult to solve this equation directly because c_a depends on k, cf. equation (2.9). Therefore, we work out the explicit dependence defining $z = \sqrt{c_a}\,x$ such that

$$\hat{n}(z) = \sqrt{c_a}\frac{z^2}{z^3/3 - z + \kappa} \qquad \text{where } \kappa = c_a^{3/2}k$$

and thus it is worthwhile to introduce the function

$$\mathcal{Z}_i(\kappa) = \int \frac{z^{2+i}}{z^3/3 - z + \kappa}\,\mathrm{d}z.$$

2.2.2. Determining the Parameters

Also, we calculate using this explicit $\hat{n}(x)$ the volume V_{tot} and the number of droplets N, see equations (2.8) and (2.7a):

$$N = \int \hat{n}(x)\,\mathrm{d}x = \int \frac{x^2}{x^3/3 - x/c_a + k}\,\mathrm{d}x = \int \hat{n}(z)\,\mathrm{d}z = \mathcal{Z}_0(\kappa) \tag{2.14}$$

$$V_{\text{tot}} = t \int \frac{x^5}{x^3/3 - x/c_a + k}\,\mathrm{d}x = t\, c_a^{-3/2}\, \mathcal{Z}_3(\kappa) \tag{2.15}$$

Moreover, we insert N using equation (2.14) in the formula for the overall droplet volume (2.5b). This expression for V_{tot} has to be the same as in (2.15), i.e.

$$\begin{aligned} & t\, c_a^{-3/2}\, \mathcal{Z}_3(\kappa) \stackrel{!}{=} 3\, \mathcal{Z}_0(\kappa)\,(1-k)\,t \\ \Leftrightarrow \quad & 3\,(1-k)\, c_a^{-3/2} = \frac{\mathcal{Z}_3(\kappa)}{\mathcal{Z}_0(\kappa)} \\ \Leftrightarrow \quad & c_a = \left(\frac{\mathcal{Z}_3(\kappa)}{3\mathcal{Z}_0(\kappa)} + \kappa \right)^{2/3} \\ & k = \kappa\, c_a^{-3/2} \end{aligned} \tag{2.16}$$

This means for a given κ we can calculate k and c_a, in figure 2.1 we show the just calculated dependence (2.16).

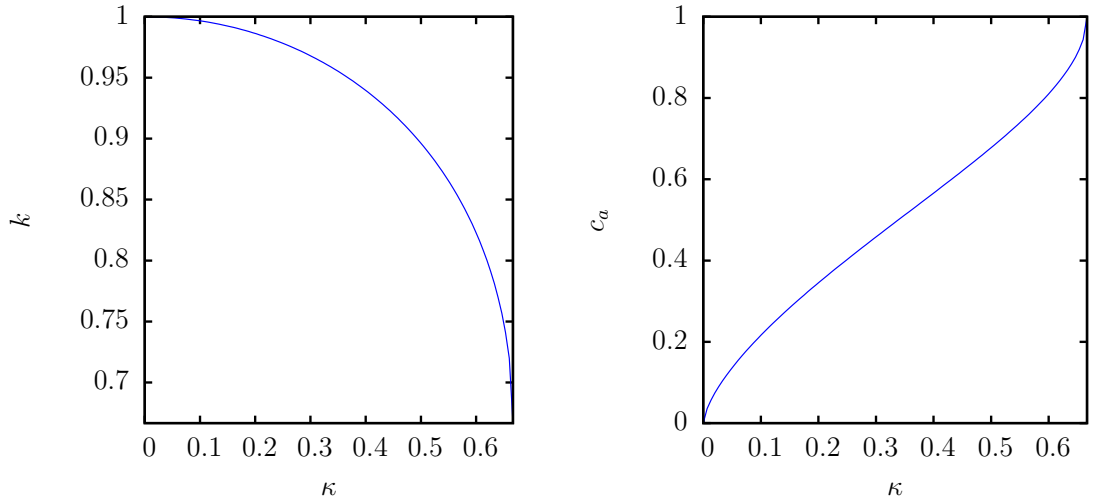

Figure 2.1.: Dependence of k and c_a on κ.

2.2.3. Domain of the Distribution

Firstly, we are interested in the domain of $\hat{n}(z)$ that determines the limits of the integration in $\mathcal{Z}_i(\kappa)$. Analyzing the denominator of $\hat{n}(z)$

$$\mathfrak{D}_\kappa(z) := z^3/3 - z + \kappa$$

one sees that depending on κ the polynomial has only real zeros if $\left|\frac{3}{2}\kappa\right| \leq 1$ which is the case we investigate. These zeros are determined by

$$\hat{z}_i = 2\cos\left(\frac{1}{3}\arccos\left(-\frac{3\kappa}{2}\right) - i\frac{2\pi}{3}\right) \quad \text{for} \quad i = 0, 1, 2\,.$$

Defining $\mathcal{S}(\kappa) := \hat{z}_0$ one can inspect by symmetry arguments that $\hat{z}_2 = -\mathcal{S}(-\kappa)$ and $\hat{z}_1 = -\hat{z}_0 - \hat{z}_2$ [11]. As z is always positive the value of the smallest positive zero $\hat{z}_1$ locates the singularity z_m of $\hat{n}(z)$:

$$z_m = 2\left[\cos\left(\frac{1}{3}\arccos\left(\frac{3\kappa}{2}\right)\right) - \cos\left(\frac{1}{3}\arccos\left(-\frac{3\kappa}{2}\right)\right)\right]. \tag{2.17}$$

So the considered domain of $\hat{n}(z)$ is $\mathbb{D} = \{z \in \mathbb{R} \mid 0 \leq z \leq z_m\}$ and thus the limits of the integral are zero and z_m. Consequently, $\mathcal{Z}_i(\kappa)$ diverges and we encounter a problem regarding equation (2.16), c_a seems to diverge. Therefore, we expand $\mathcal{Z}_0(\kappa)$ and $\mathcal{Z}_3(\kappa)$ in a Laurent series in zeroth order since this part diverges. Thus, to calculate c_a we need

$$\frac{\mathcal{Z}_3(\kappa)}{\mathcal{Z}_0(\kappa)} = \frac{z_m^5 \int_0^{z_m} \mathfrak{D}_\kappa(z)^{-1}\,\mathrm{d}z}{z_m^2 \int_0^{z_m} \mathfrak{D}_\kappa(z)^{-1}\,\mathrm{d}z} = z_m^3 \quad \Rightarrow \quad c_a = \left(\frac{z_m^3}{3} + \kappa\right)^{2/3}.$$

2.3. Numerical Solution

Now that we reduced the dependence of $\hat{n}(z)$ to one parameter κ we choose some $\kappa \in [0, 2/3]$ and calculate the distribution $\hat{n}(x)$ knowing $k(\kappa), c_a(\kappa)$. Then we pick certain k and show the corresponding distribution on figure 2.2, rescaling x to $x/\overline{a}$ and defining $u := a/\overline{a}$.
We observe, that the location and amplitude of the maximum depend on k.

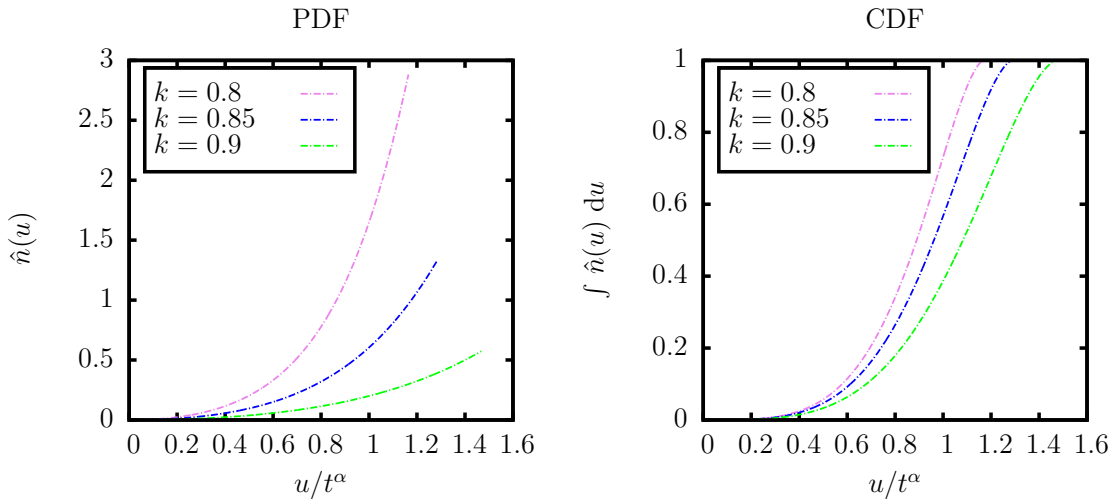

Figure 2.2.: Numerical solution for the theoretic droplet size distribution. We obtain the distribution by a scaling ansatz and choose certain values for a parameter κ that determines the $k(\kappa)$ from the surveyed differential equation. On the left, we see the distribution (PDF), on the right the cumulative distribution (CDF) is shown.

3. Time Dependence

The droplet size distributions obtained in section 2.2 appear very different from the form suggested by Lifshitz and Slyozov. In order to verify that the approximations used in the derivation hold, and to explore the transient dynamics, we employ numerical simulations. To that end, we evolve (2.4) for $N_0 = N(0) = 2000$ droplets (cf. chapter A). In the end, as both distributions describe the same physics, we expect them to be very much alike.

3.1. Evolution at Constant Temperature

We recall the results from section 2.2, and state that for an evolution at constant temperature the overall droplet volume stays constant, and it follows $\lambda = 0$ and $\alpha = 1/3, \beta = 4/3$.

3.1.1. The LS-Approximation for the Droplet Size Distribution

To find the droplet size distribution for drops that behave according to (2.3), Landau and Lifshitz worked out an analytic expression under certain assumptions [3]. Let $g(t, a)$ be such a distribution describing the density of droplets per volume. Since we look at a quench experiment, the solution is supersaturated in the beginning and afterwards no further drops are added, g obeys a continuity equation

$$\dot{g} + \frac{\partial(g\, v_a)}{\partial a} = 0.$$

Since we know the solution to the homogeneous continuity equation we obtain an explicit expression for the distribution. Adjusting length and time scales and using Taylor expansion up to second order, we can write, with the transformations $u =$

$a/a_c(t)$ and $\tau = 3\ln(a_c(t)/a_c(0))$, the differential equation as

$$\dot{u} = -\frac{1}{3u^2}\left(u - \frac{3}{2}\right)^2 (u+3).$$

Similarly, we have a continuity equation for the rescaled distribution $\phi(\tau, u)\mathrm{d}u = g(t,a)\mathrm{d}a,\ \phi = g\, a_c$. This equation is solved by $\phi(\tau, u) = Ae^{-\tau}P(u)$ where A is a constant such that $P(u)$ is normed to 1. Thus, we obtain the time invariant distribution

$$\mathrm{LS}(u) := P(u) = \begin{cases} \dfrac{3^4 e}{2^{5/3}} \dfrac{u^2 \exp[-1/(1-2u/3)]}{(u+3)^{7/3}(3/2-u)^{11/3}}, & u < \frac{3}{2} \\ 0, & u > \frac{3}{2} \end{cases}. \tag{3.1}$$

Given this distribution, the number of droplets N and the volume V_{tot} of the system can be expressed as

$$\frac{\overline{a}^3}{t} = \frac{4}{9}, \quad N = t^{-1}\int_0^\infty \hat{n}(x)\ \mathrm{d}x, \tag{3.2}$$

$$\dot{V}_{\mathrm{tot}} = \sum_{i=1}^{N} \frac{\mathrm{d}a_i^3}{\mathrm{d}t} = 3\sum_{i=1}^{N} a_i^2 \dot{a}_i = 3\sum_{i=1}^{N}\left(\frac{a_i}{\overline{a}} - 1\right) = 3N(1-1) = 0. \tag{3.3}$$

3.1.2. Consistency checks

In order to find out whether the results of the simulations are consistent with the LS-theory we performed a number of consistency checks. An important assumption of the LS-theory is the volume conservation. In our numerical treatment we expect the volume fraction of droplets $\sum_i a_i^3/V_{\mathrm{sys}}$ to be constant, where V_{sys} is the system volume. Apart from tiny discontinuities where the system size is changed[1] this value is indeed constant, cf. figure 3.1. Moreover, the theory predicts that $\overline{a}^3 \propto t$, see (3.2). This is also captured in the simulation, cf. figure 3.2.

[1] This is due to the way we change the system size, see A.

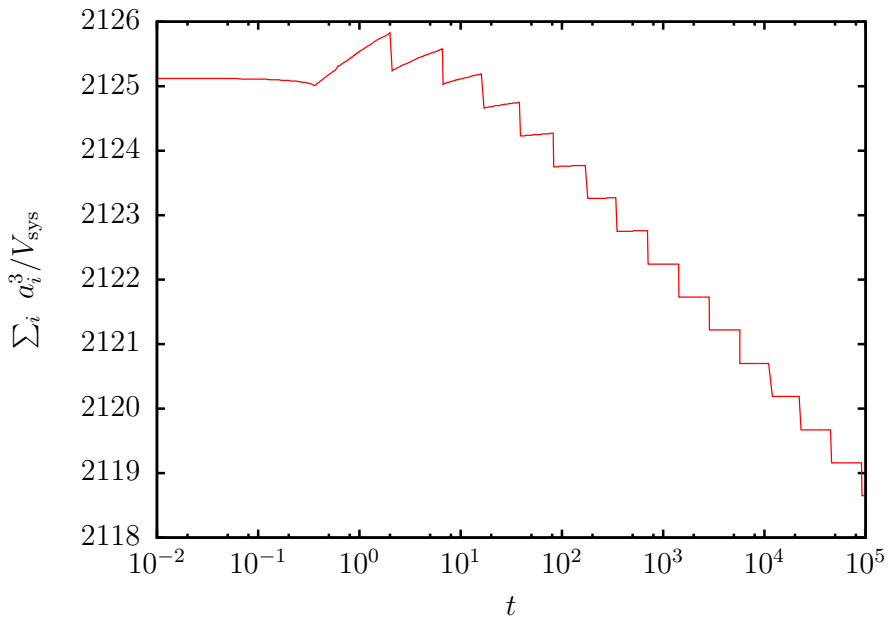

Figure 3.1.: Time dependence of $\sum_i a_i^3/V_{\mathrm{sys}}$. After a crossover time, when the system is assimilated and the initial conditions play no role anymore, we see that apart from small discontinuities the volume is indeed constant.

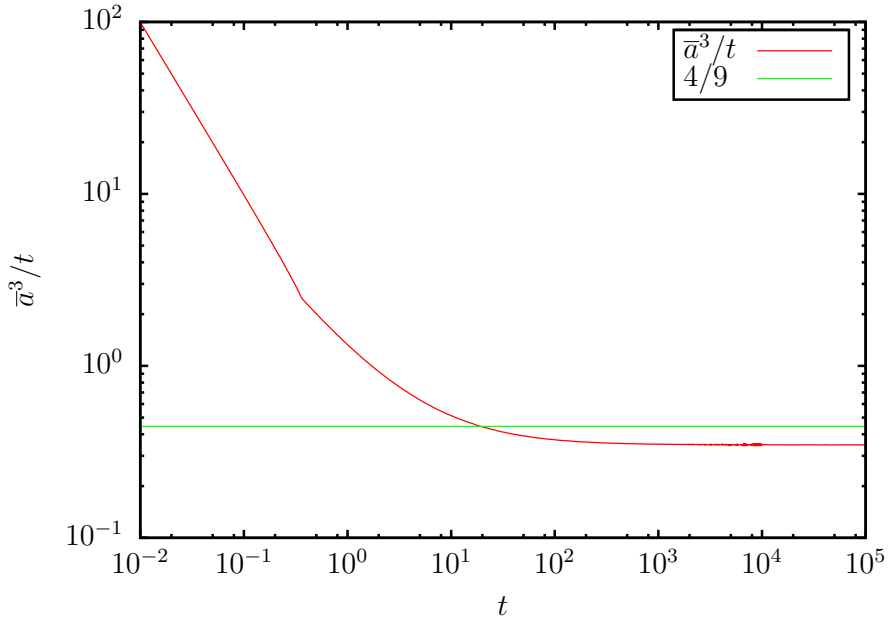

Figure 3.2.: Time dependence of average over all droplets. After the system assimilated the quantity $\overline{a}^3/t$ is constant as predicted.

Furthermore, in LS-theory the number of droplets N depends on t like $N \propto t^{-1}$ which is observed in figure 3.3.

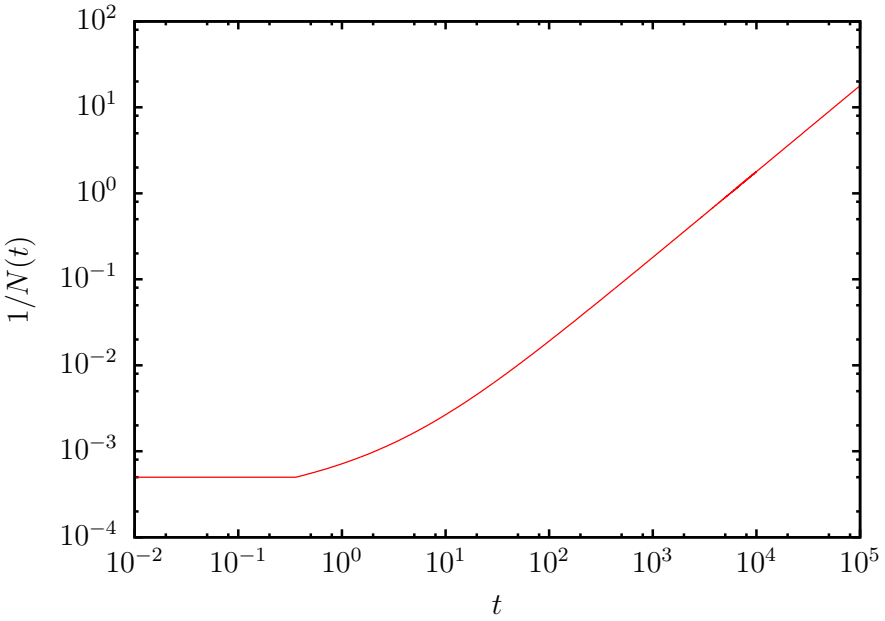

Figure 3.3.: Time dependence of number of droplets. When the crossover time is reached we verify the dependence $N \propto t^{-1}$.

3.1.3. Convergence to a Scaling Solution

The droplets evolve according to (2.3) and we will obtain the discrete droplet size distribution by our simulation. Resulting from the previous considerations we expect a time-invariant scaling distribution.
First of all, we may ask whether the initial radii affect the asymptotic size distribution in the simulation. So we choose two vastly different initial conditions:

A) Firstly, we investigate uniformly distributed radii around 1,

$$a_i(0) = 0.75 + \frac{i}{N_0 - 1} \cdot 0.5, \quad i = 0, \ldots, N_0 - 1. \tag{3.4a}$$

The time evolution of the resulting droplet size distribution for this uniform initial distribution is shown on figure 3.4. For $t > 10^3$ the PDF converges to a constant shape. The characteristic cut-off at an asymptotic value u_a can be seen, although it differs a lot from LS(u), where no sharp maximum is observed.

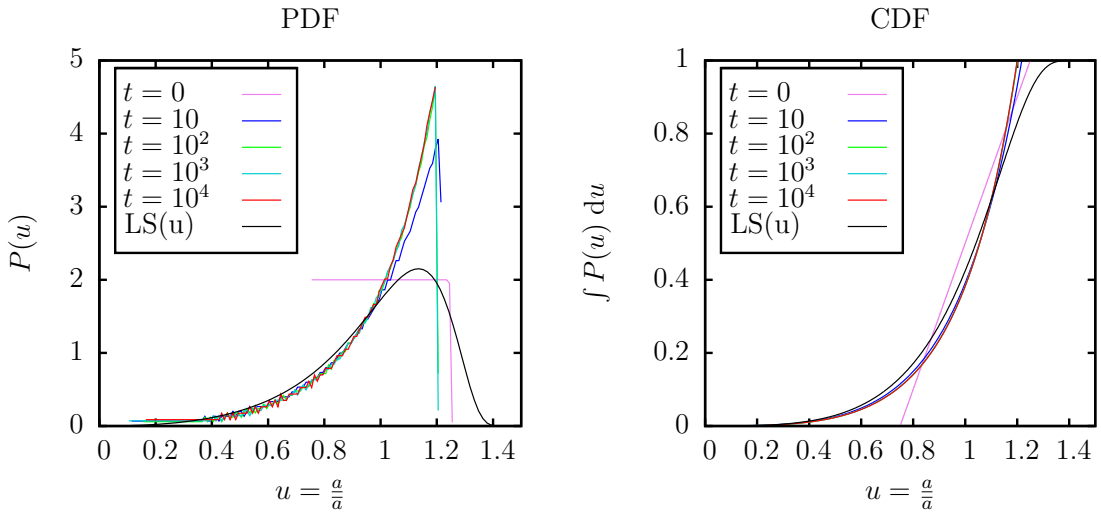

Figure 3.4.: Size distribution for a system with constant temperature after time t for uniformly distributed initial radii (3.4a). On the left panel we see a distribution (PDF) that we obtained by binning the values for u with a bin width of 0.01. However, as the shape close to the sharp maximum is strongly affected by the chosen bin width, it is more convenient to study the cumulative distributions. The right panel shows the cumulative distribution (CDF).

B) Secondly, we choose as initial distribution a tanh-distribution with the same initial average as before, i.e.

$$a_i(0) = 1 + \tanh\left(\frac{2i - N + 1}{N - 1}\right)/4, \quad i = 0, \ldots, N_0 - 1 \tag{3.4b}$$

which gives us insight into the fate of initial bimodal distributions, as they have been observed in clouds [8]. Figure 3.5 shows the evolution of this distribution.

The rate of convergence to a steady scaling solution apparently does not differ for both distributions.

However, eventually the asymptotic shape of the distributions is the same, cf. figure 3.6. Unfortunately, the asymptotic distribution differs substantially from both, the prediction of LS and the solution obtained in section 2.3. The origin of this discrepancy is unclear as yet.

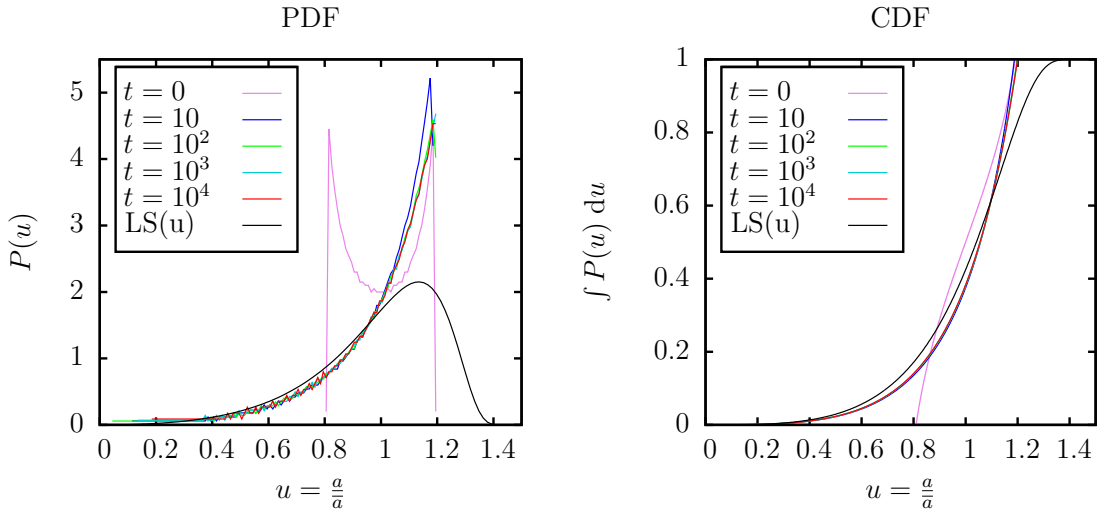

Figure 3.5.: Size distribution for a system with constant temperature after the time t for tanh-distributed initial radii (3.4b). On the left the binned values with bin width 0.01 are shown, on the right we see the cumulative distribution. The characteristic cut-off is recognizable.

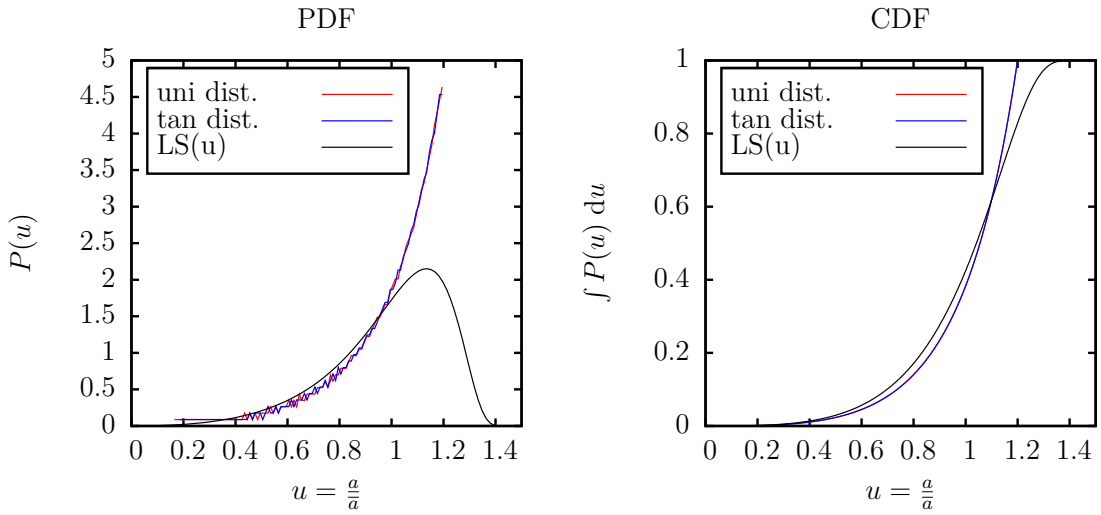

Figure 3.6.: Comparing both initial conditions at time $t = 10^4$. The PDF is binned with bin width 0.01. The distributions converge and have the same asymptotic shape.

3.2. Evolution with Constant Change of Overall Droplet Volume

We argued in 2.2 that the volume depends linearly on time for $k \neq 1$. In that situation equation (2.4) refers to a system where a constant heating or cooling rate is applied, the overall droplet volume is *not* conserved. This is reproduced by figure 3.7, showing the evolution of the droplet volume fraction $\sum_i a_i^3/V_{\text{sys}}$.

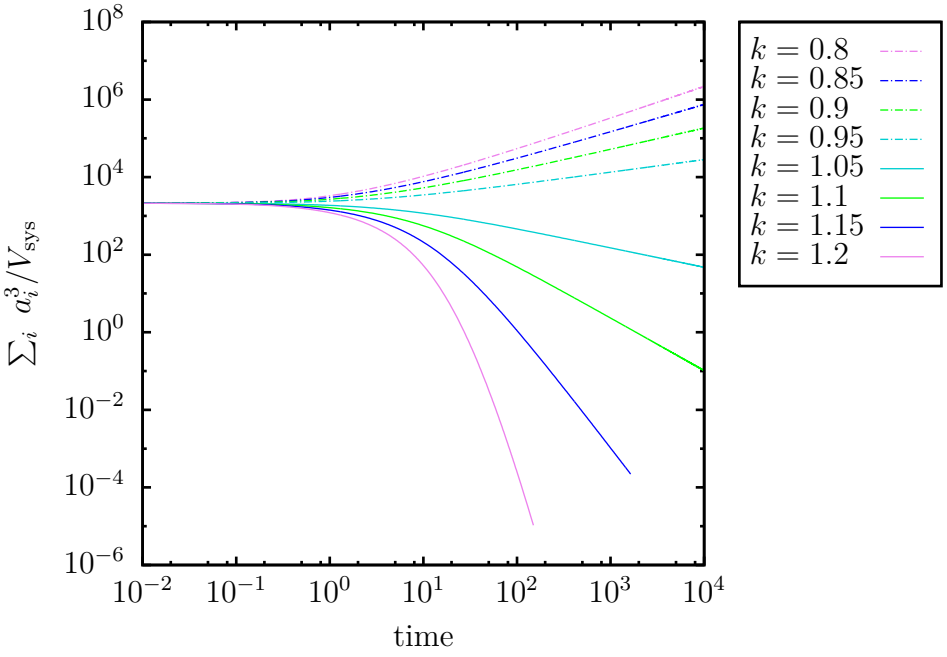

Figure 3.7.: The volume fraction $\sum_i a_i^3/V_{\text{sys}} = V_{\text{tot}}/V_{\text{sys}}$ for every k. For $k < 1$ this value increases and for $k > 1$ it decreases, as predicted by (2.5a).

We saw that in the scaling regime $N = \text{const.}$ is valid, see equation 2.8 with $\alpha = \beta = 1/3$. Thus, in view of equation (2.5a) it holds

$$\sum_i a_i^3 \cdot \frac{1}{3N(1-k)t} = \text{const.}$$

what we also obtain from the simulation, see figure 3.8. For $k = 1$ we already discussed in 3.1.2 that the volume is constant. If simulation and theory worked right, for arbitrary k the value $\sum_i a_i^3 \cdot \frac{1}{3N(1-k)t}$ should be constant.

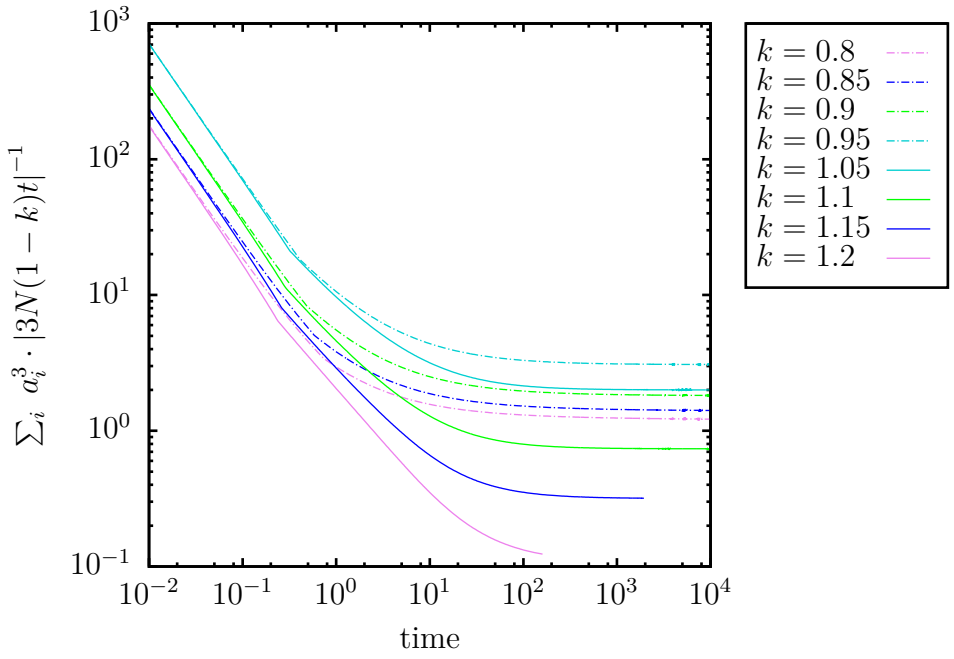

Figure 3.8.: Rescaled volume for constant change of temperature. According to (2.5a) we see that the total volume of the system goes as $V_{\text{tot}} \propto 3N(1-k)t$, motivating the division of the volume of droplets in the whole simulated system by $|V_{\text{tot}}|$ in order to use a log scale because for $k > 1$ for the volume holds $V_{\text{tot}} < 0$. We observe that the asymptotic value is indeed constant for $k \neq 1$.

We observe that the values before $t = 10^2$ are not constant because the system approaches the LS-regime, the steady state is seen after a crossover time t_{cr} and thus simulation and theory agree. For some $k > 1$ we observe that the simulation stops before the integration time passed. So in these cases the volume decreased to zero. This happens abruptly from one time step to another as we choose a fixed step size.

The convergence of N to a constant value can be studied relating the volume to the number of droplets using equation (2.5b) by analyzing the time dependence of

$$\frac{V(t) - V_0}{3(1-k)Nt} \,. \tag{3.5}$$

This analysis is shown in figure 3.9.
The expectation is fulfilled, after the crossover time N is constant.

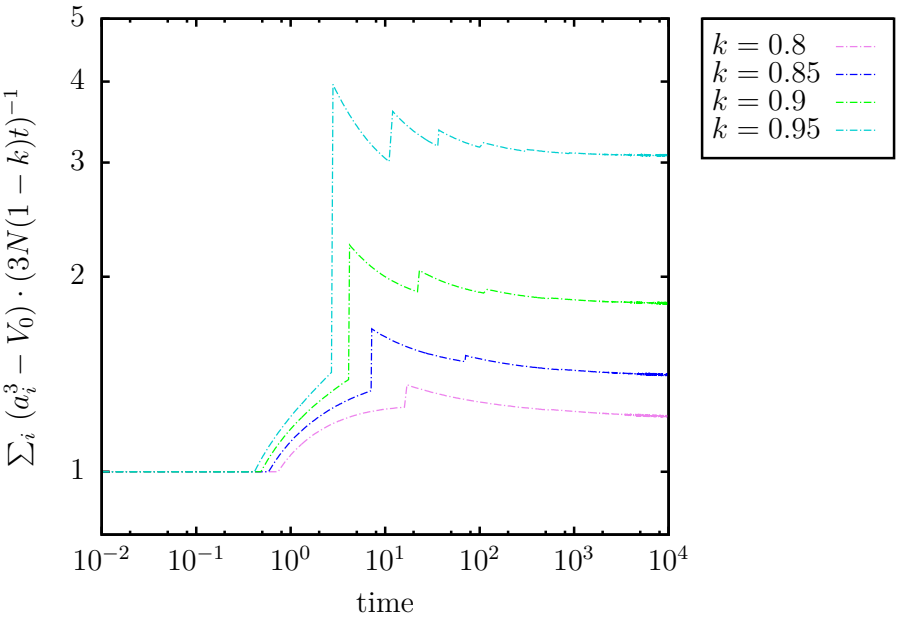

Figure 3.9.: Rescaled volume evolution. Regarding (3.5) we rescale the volume and observe a constant asymptotic value. This covers that N is constant.

Besides the evolution of the droplet number density, we are also interested in the size distributions (cf. figure 3.10).

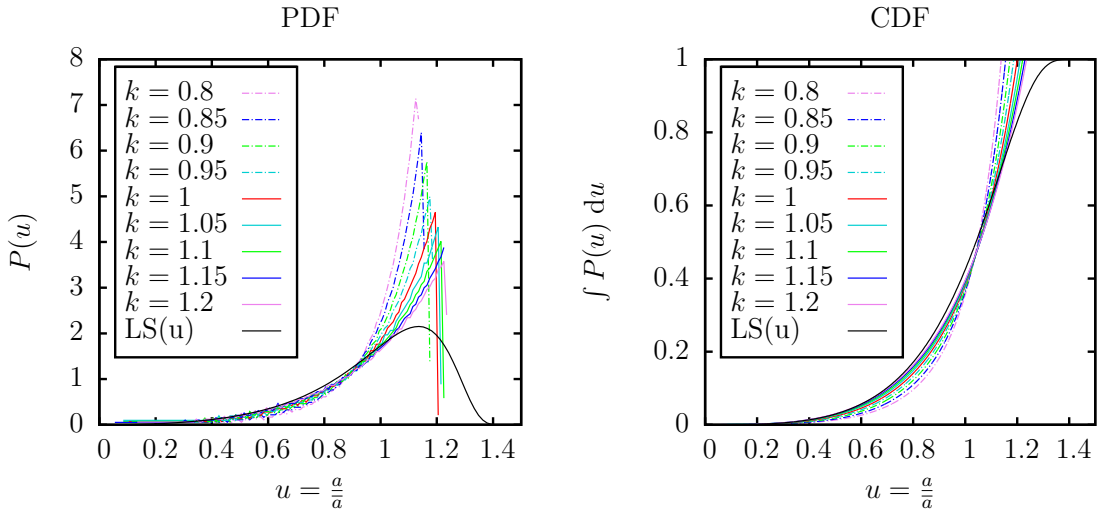

Figure 3.10.: The k-dependence of the asymptotic droplet size distribution for constant driving at time $t = 10^4$. Again, the distributions $P(u)$ are binned with a bin width of 0.01. The case $k = 1$ is inserted to provide a comparison of the results. The position and height of the maximum depend strongly on k.

For every k we observe that the maximum is located somewhere else, but the sharp cut-off stays the same. For increasing k it moves to the right and takes smaller values. As for $k = 1$ we observe a sharp cut-off of the distribution for droplet sizes of a few percent ($k = 0.8$) up to 20% ($k = 1.2$) larger than $\overline{a}$.

Finally, we explore the evolution of $\overline{a}^3/t$, for different k the value $\overline{a}^3/t$ is asymptotically constant in accordance with the prediction obtained in section 2.2 (cf. figure 3.11).

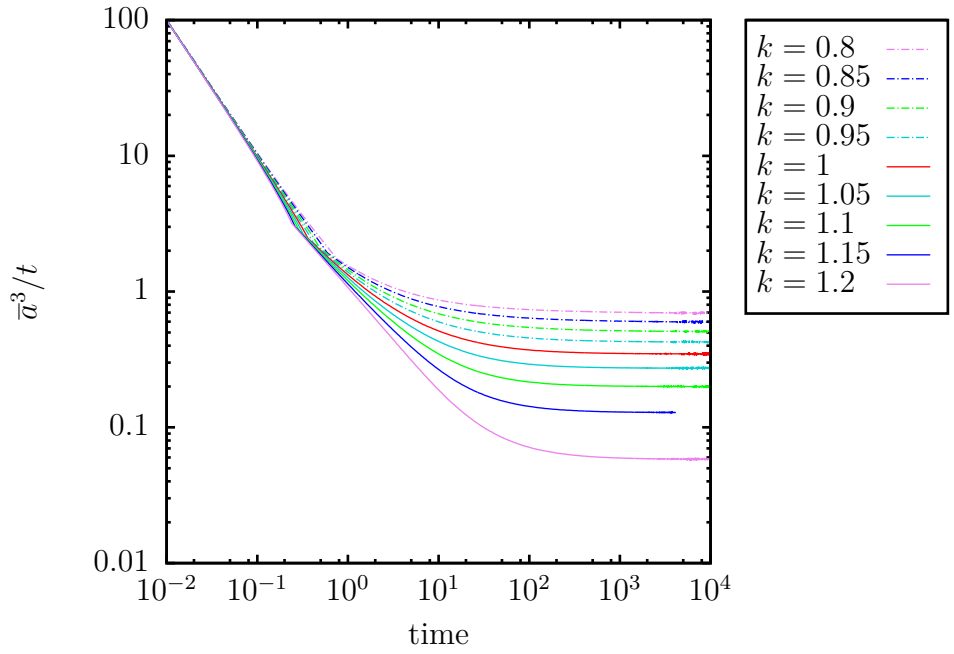

Figure 3.11.: Value of $\overline{a}^3/t$ for several k. After the crossover time this value is constant for each k, derived in (2.9) with $\alpha = 1/3$ independent on the choice of k. Again, for $k > 1$ some curves are not defined until $t_{\text{end}} = 10^4$ because the volume decreased to zero.

Regarding this, we state that the asymptotic values of the curves are different.

We summarize the dependence of $\overline{a}^3/t$ on k in figure 3.12 with $t_{\text{end}} = 10^4$, defining

$$\mathrm{Dr}(t) := \frac{\overline{a}^3}{t}$$

and a discrete crossover function $A(k)$ that contains the k-dependence of $\overline{a}^3/t$. We

obtain $A(k)$ by a fitted curve

$$\overline{a}^3/t = A(k) + \frac{\text{const.}}{t} \ .$$

This curve shape arises from figure 3.11 where we see

$$\overline{a}^3/t \propto 1/t \text{ for small } t \text{ and } \overline{a}^3/t = \text{const. for } t > t_{\text{cr}}.$$

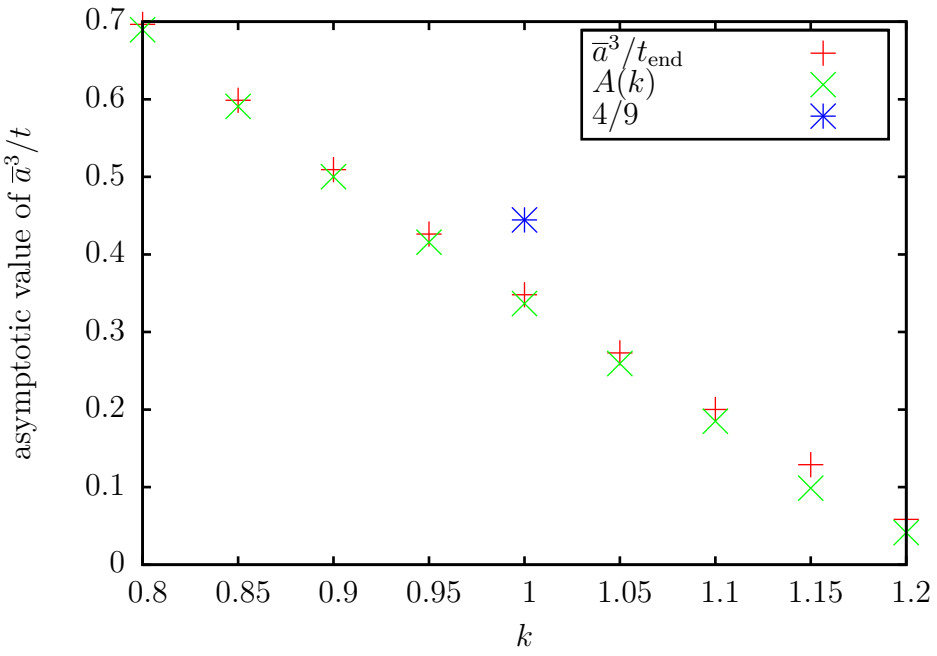

Figure 3.12.: Summing up the dependence of asymptotic value of k after $t_{\text{end}} = 10^4$. The star at $(1, 4/9)$ marks the prediction of LS-theory. The asymptotic values from the simulation is shown for two different calculations. The asymptotic value of a fitted curve at t_{end} is defined as $A(k)$.

We compare the theoretic value derived by Lifshitz and Slyozov with the values we obtain from figure 3.11 depending on whether we choose the value $\overline{a}^3/t_{\text{end}}$ or a value $A(k)$ from a fitted curve and state, that they differ. As the end value oscillates due to numerical errors, the results from the fitted curve are more reliable.

Using the calculated $A(k)$ we can shift the curves from figure 3.11 to lie on approximately one curve by rescaling the time to $t' = t \cdot A(k)$ for every considered k.

So the transformed asymptotic value is

$$\mathrm{Dr}(t') = \mathrm{Dr}(t \cdot A(k)) = \overline{a}^3/(t \cdot A(k)). \tag{3.6}$$

Thus, every asymptotic value of $\mathrm{Dr}(t')$ is close to one and the curves join. Figure 3.13 shows the result.

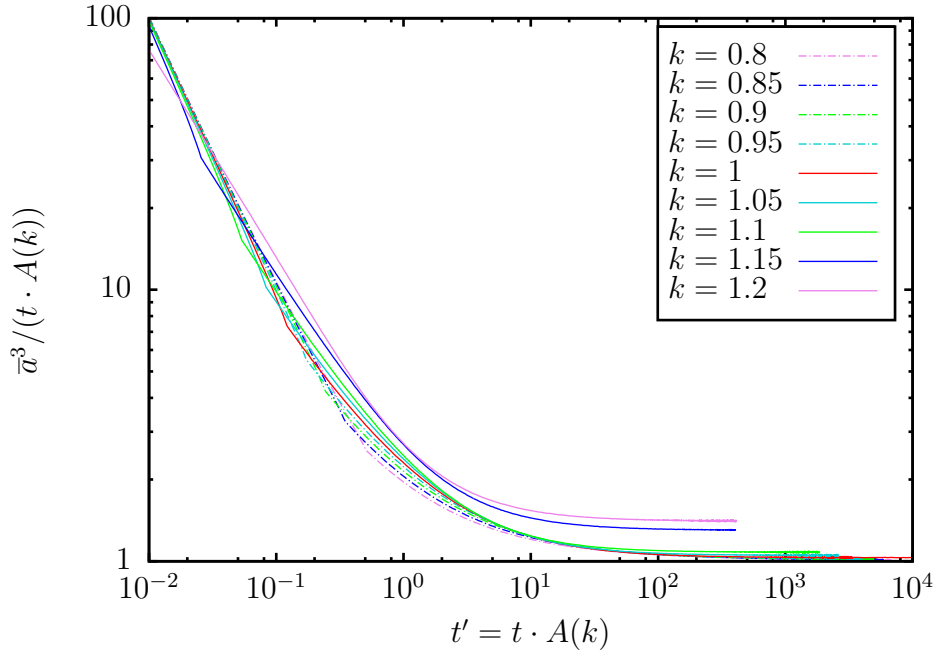

Figure 3.13.: Rescaling the time t to $t' = t \cdot A(k)$. $A(k)$ is obtained from the fitted curve. The curves for different k thus result in one curve due to $\mathrm{Dr}(t') \approx 1$.

The fit provides an excellent data collapse for $k < 1$, where the droplets grow on the average. On the other hand, the results are not reliable for $k > 1$, because all droplets disappear from the system in a finite time when the temperature is moved towards the single-phase region.

We also modeled an oscillating change of temperature. Due to more parameters the simulation time is longer, preliminary results are discussed in chapter B.

4. Effects of Droplet Sedimentation

4.1. Extending the Model

Now we go back to the differential equation (2.3) derived by Lifshitz and Slyozov. For this differential equation the volume is conserved as no droplets are added or taken away with size greater than zero. But we are interested in the growth of droplets by sweeping up smaller ones, i.e. cloud droplets that catch smaller drops and coalesce with them. When droplets sediment they collide with some efficiency with smaller droplets [9]. This accelerates the growth of the big droplets. Let the jth droplet sweep up the ith droplet. We take into account the collision contribution $\frac{\varepsilon}{V_{\text{sys}}}(a_i+a_j)^2$ for some ε[1], comprising the cross-section $(a_i+a_j)^2$ and the difference of the Stokes' sedimentation velocities[2] $\propto a_i^2 - a_j^2$. Also, the volume of the jth droplet $\propto a_j^3$ is considered. By this sweeping of the ith drop the volume of the bigger droplet with radius a_j increases at a rate

$$S(i) = \frac{\varepsilon}{V_{\text{sys}}} a_j^3 \left(a_i + a_j\right)^2 \left(a_i^2 - a_j^2\right)$$

where we absorb all constants in ε. This parameter determines whether we reach the crossover time before the finite time runaway due to the sweeping. A convenient choice for the simulation is $\varepsilon = 10^{-6}$. The overall volume change for the jth droplet is then given by the sum over all contributions $S(i)$ by smaller droplets $a_i < a_j$. This leads to differential equations of the form

$$\dot{a}_i = \left(\frac{a_i}{\overline{a}} - k\right) \cdot \frac{1}{a_i^2} + \frac{\varepsilon}{a_i^2 V_{\text{sys}}} \sum_{j=1}^{i} a_j^3 \left(a_i + a_j\right)^2 \left(a_i^2 - a_j^2\right) \tag{4.1}$$

The collisions enhance the growth of big droplets. Small droplets however disappear

[1] We will discuss the exact value of ε later.

[2] The Stokes' velocity is defined to be $v_s = \frac{2}{9}\frac{\Delta\rho}{\mu} g\, a^2$ with radius a, dynamic viscosity μ, gravitational acceleration g and density difference $\Delta\rho$ between particles and fluid.

during this process with the probability $P_{\text{die}}(a_i)$ by being swept up. Similar to the above considerations we can calculate the probability do die. To that end we account for the droplets that are bigger than the ith droplet:

$$P_{\text{die}}(a_i) = 3\ \Delta t\ \frac{\varepsilon}{V_{\text{sys}}} \cdot a_i^3 \sum_{j=i}^{N} (a_i + a_j)^2 (a_j^2 - a_i^2) \tag{4.2}$$

For the parameters $\Delta t = 10^{-3}, \varepsilon = 10^{-6}$ in our simulation the Metropolis criterion [1] is fulfilled, the probability for a transition, i.e. a droplet removal, is always smaller than 1, even smaller than 2/3. So (4.2) is indeed a probability.

4.2. Evolution at Constant Temperature

In order to look at the case of constant temperature ($k = 1$) we consider the probability to die (4.2) by being collected by a bigger droplet and the differential equations

$$\dot{a}_i = \left(\frac{a_i}{\overline{a}} - 1\right) \cdot \frac{1}{a_i^2} + \frac{\varepsilon}{a_i^2 V_{\text{sys}}} \sum_{j=1}^{i} a_j^3 \left(a_i + a_j\right)^2 \left(a_i^2 - a_j^2\right).$$

We first prove that for $k = 1$ the volume is conserved. By equating

$$\frac{\mathrm{d} \sum_{i=1}^{N} a_i^3}{\mathrm{d}t} = 3 \sum_{i=1}^{N} \left(\frac{a_i}{\overline{a}} - 1\right) + 3 \frac{\varepsilon}{V_{\text{sys}}} \sum_{i=1}^{N} \sum_{j=1}^{i} a_j^3 \left(a_i + a_j\right)^2 \left(a_i^2 - a_j^2\right)$$

we find that the first term is zero and the second term is composed of a contribution of each droplet plus the contributions of smaller droplets. This change represents diffusive exchange with the environment, which does not affect the volume at a fixed temperature, and growth by collection of smaller droplets. In addition, we must consider the probability to die for each droplet, that is composed of the sum of contributions of bigger droplets:

$$\Delta \left(\sum_{i=1}^{N} a_i^3\right) = 3 \Delta t \frac{\varepsilon}{V_{\text{sys}}} \sum_{i=1}^{N} a_i^3 \sum_{j=1}^{i} \left(a_i + a_j\right)^2 \left(a_i^2 - a_j^2\right).$$

Rearranging the sums one observes that the growth and death contributions balance each other such that the volume fraction of droplets is conserved. Within the numerical error margins this is supported by figure 4.1.

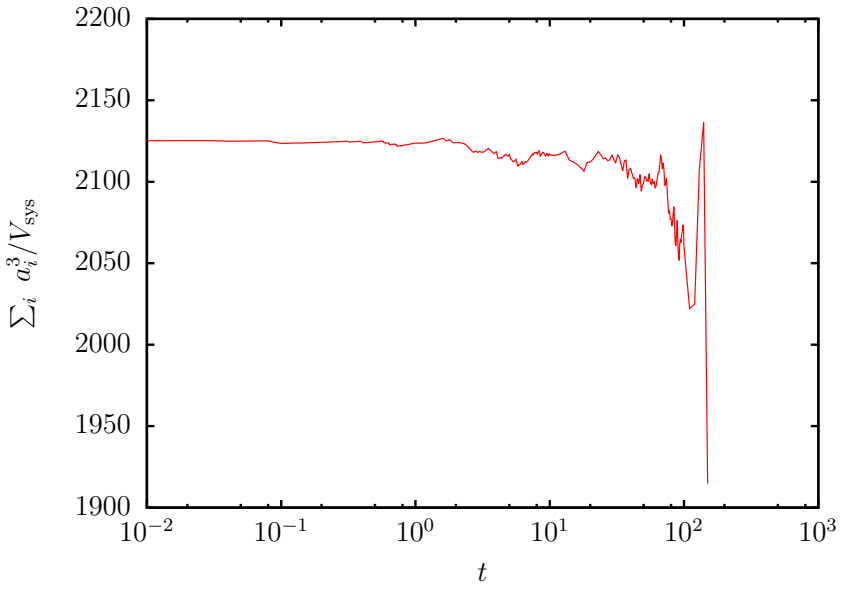

Figure 4.1.: Volume in the system that is driven by droplet sedimentation. Similar to the Lifshitz-Slyozov theory the volume $\sum_i a_i^3/V_{\mathrm{sys}}$ is conserved apart from the time when the runaway sets in. By applying (2.3) and regarding the efficiency of sedimenting and vanishing droplets in the same way the volume is conserved.

Another question is what the size distributions look like. In figure 4.2 one can see that the maximum evolving in time first decreases, then increases again for smaller values of u and finally leads to a finite time runaway for increasing t, meaning that after a certain time the number of big droplets and thus also the droplet volume diverges.

We saw that in LS-theory for the number of droplets holds $N(t) \propto t^{-1}$. In the case of droplet sedimentation and sweeping of smaller droplets the number of droplets evolves in time like shown in figure 4.3. After the crossover time the predictions of LS-theory are observed followed by the finite time runaway.

Also, the value of $\overline{a}^3/t$ evolves in time and is shown on figure 4.4. Similar to the number of droplets the evolution of the value $\overline{a}^3/t$ can be separated in three parts. The crossover time is needed to overcome initial conditions and is an approach to LS-theory, while in a small section we observe that $\overline{a}^3/t$ is constant like predicted, then followed by the finite time runaway.

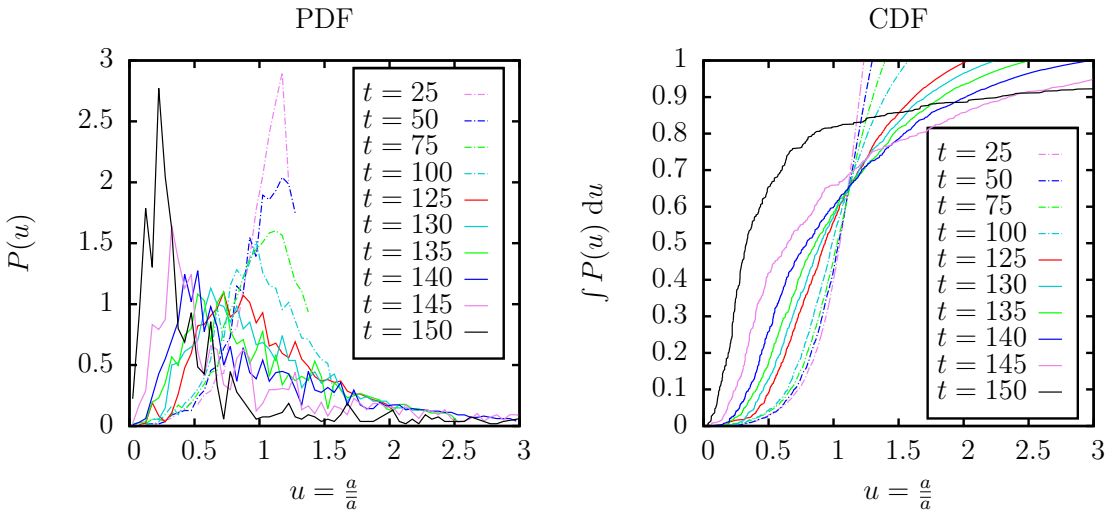

Figure 4.2.: Size distributions for droplet sedimentation, taking the survival rate of small droplets into account. Again, $P(u)$ is binned with bin width 0.01. The finite time runaway is best seen for long tails in CDF beyond $t = 125$. For $t > 140$ a slight shape of a second maximum can be seen, the existence of the second maximum was measured [8].

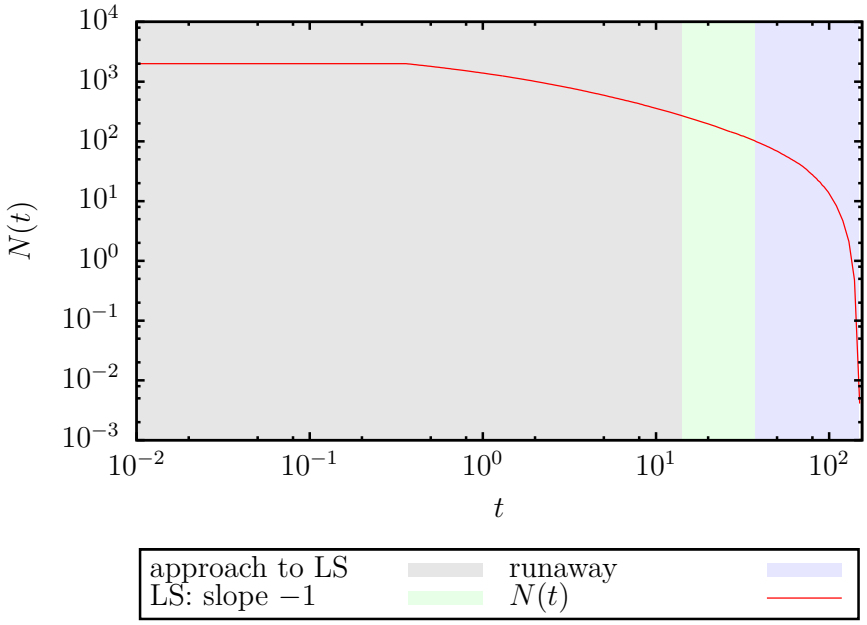

Figure 4.3.: Number of droplets depending on time for the sweeping of small droplets. After the crossover time in a small area we observe the power law of N that arose in the Lifshitz-Slyozov theory, stating $N \propto t^{-1}$. For increasing time we observe the finite time runaway.

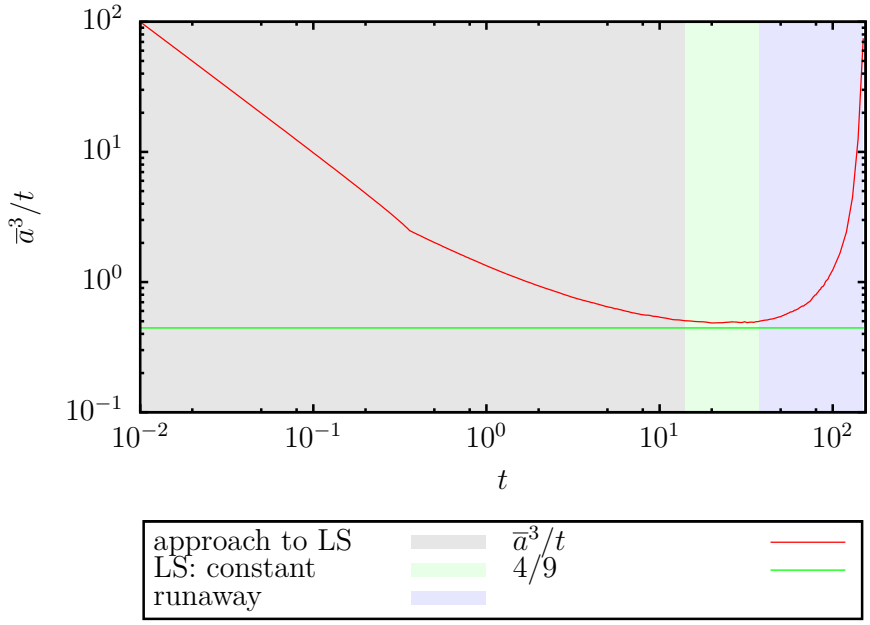

Figure 4.4.: Evolution of $\overline{a}^3/t$ for droplet sedimentation including droplet removal. The value 4/9 from LS-theory is also shown. Until the crossover time is reached the system approaches the LS-regime, then the constant value of $\overline{a}^3/t$ is observed and diverges in the end, due to the finite time runaway.

4.3. Evolution with Constant Driving

Concerning the droplet sedimentation we found a model that extends the existing one presented by Lifshitz and Slyozov. Regarding the previous chapters it is convenient to ask now what happens if we add a driving force to the new model. Again, we choose $k \in [0.8, 1.2]$ to see what happens to the characteristic quantities of the system, taking the death rate and the volume gain by sweeping into account. So we now survey (4.1) including the probability to die.
We use the already defined and calculated discrete function $A(k)$ that yields the asymptotic value of $\overline{a}^3/t$. Again we rescale the time to be $t \cdot A(k)$. In section 4.2 we saw that for $\varepsilon = 10^{-6}$ the time range reproducing LS-theory is very small. Now we want to support the thesis that the length of the time span of LS-theory depends on ε. In order to do so, we look for several ε at the rescaled plot of $\overline{a}^3/t$ and obtain figure 4.5. To compare the value for different ε for a certain k we plot figure 4.6.

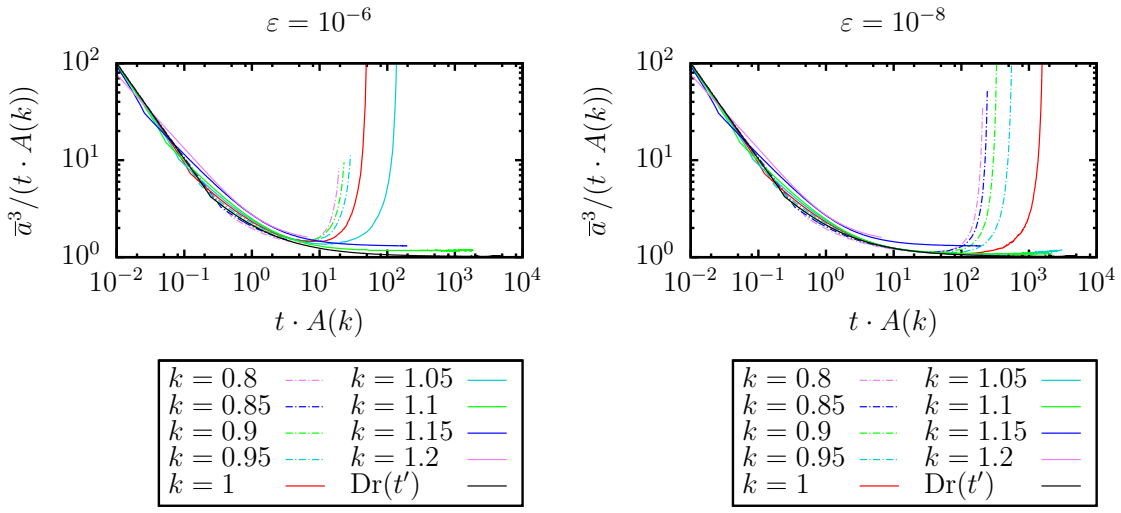

Figure 4.5.: Evolution of $\overline{a}^3/(t \cdot A(k))$ for different k. We rescale the time to $t' = t \cdot A(k)$ and again all curves merge apart from the point where they reach the regime of the runaway. We included one curve $\mathrm{Dr}(t')$ from figure 3.13 to compare the evolution to the LS-dominated part.

This shows that the smaller ε is, the bigger is the time span where LS-theory is valid.

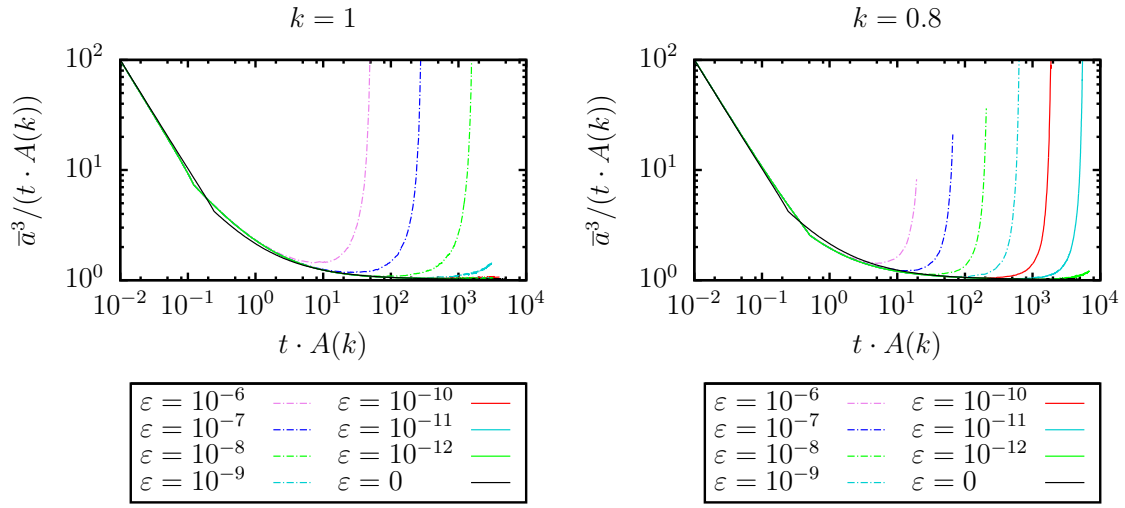

Figure 4.6.: Evolution of $\bar{a}^3/(t \cdot A(k))$ for different ε. Rescaling the time, all curves merge until they reach a singular value due to the finite time runaway. We included the case $\varepsilon = 0$ from figure 3.13.

5. Conclusion & Outlook

5.1. Adaption to Real Physics

Starting with a well-known approximation for droplet growth at constant temperature, adapting this model to more general systems that are driven by a certain change of temperature, we finally ended up with a model that describes the real volume gain and droplet removal one observes in experiments. The consistency checks for the quantities in LS-theory went very well. But still we cannot explain the sharp cut-off in the droplet size distribution from figure 3.4, neither why the distribution derived in section 2.2 fits neither to the LS-distribution nor to the simulated one. A Perl script without a system resize algorithm reproduced distributions similar to those in the discussed simulation, see A, with the same cut-off.
In section 3.2 we found out, that, after the crossover time, the number of droplets and the total volume evolve like derived in 2.2.
In the excursion we found a simple connection between the droplet growth in a general system and the adaption to clouds. ???? Whether there will be a constant slope for the volume evolving in time will then be known.

5.2. Comparing to Measurements

In their experiment Lapp et. al measure the droplet size distribution as the volume density $a^3\ f(a)$ where $f(a)$ is the number density, so we reproduce these distributions for the findings of the preceding section and obtain figure 5.1. We compare this to the measurements shown in figure 5.2.

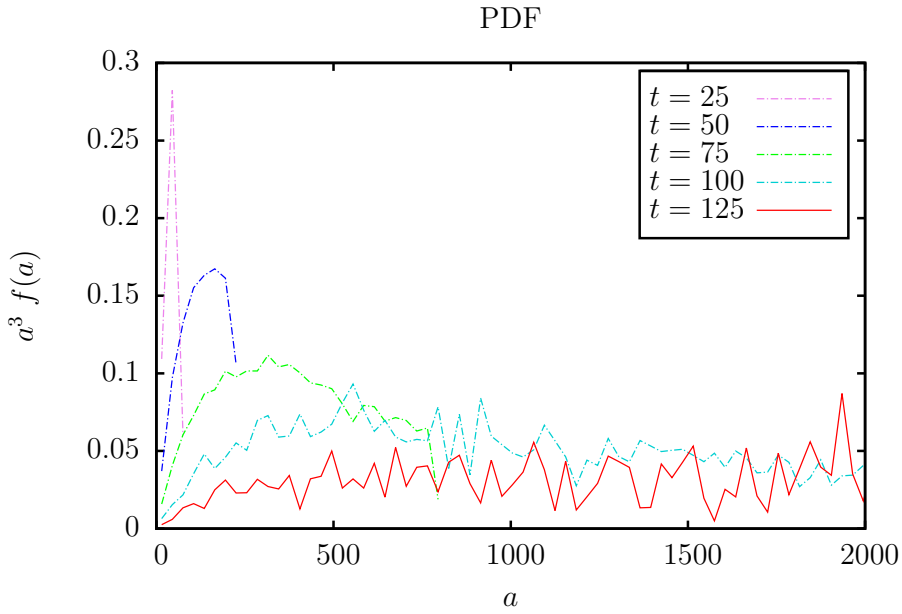

Figure 5.1.: Distribution for droplet sedimentation. To compare the data of the simulation to the experiments we look at the volume density distribution.

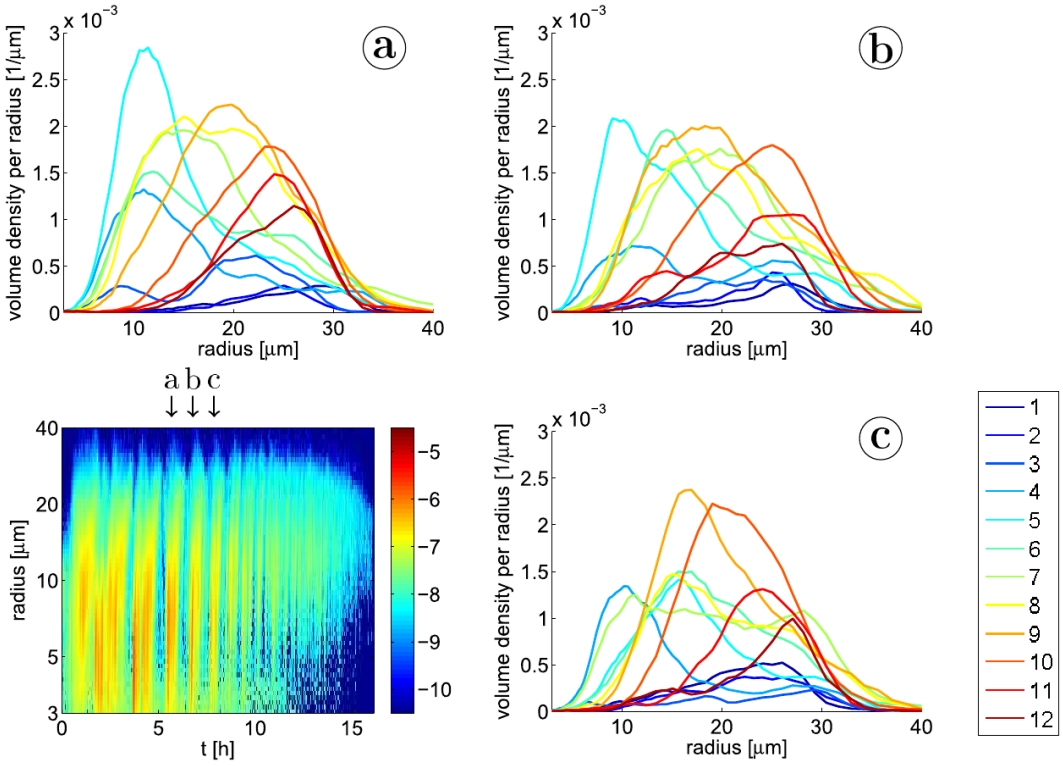

Figure 5.2.: Experimental data from Lapp et. al [7]. In the bottom left corner the evolution of the droplet size distribution is shown. Certain oscillation periods are now picked and the volume density distribution for the fourth, the fifth and the sixth oscillation are shown in a, b, c. The different colors account for a different time in one of these oscillation periods.

Similar to the experimental data, the maximum evolves in time to bigger droplet radii and the distribution broadens. But since the volume diverges for increasing time the simulated data does not correspond to the experimental findings.

5.3. Comparing the Variants to Obtain a Distribution

In the present thesis we encountered several methods to obtain the droplet size distribution of precipitation. For a constant change of temperature like in the experiments of Lapp et al. we derived a theoretic expression for the distribution, also the simulation leaded to distributions depending on k. In figure 5.3 we compare these two methods of obtaining the size distribution.

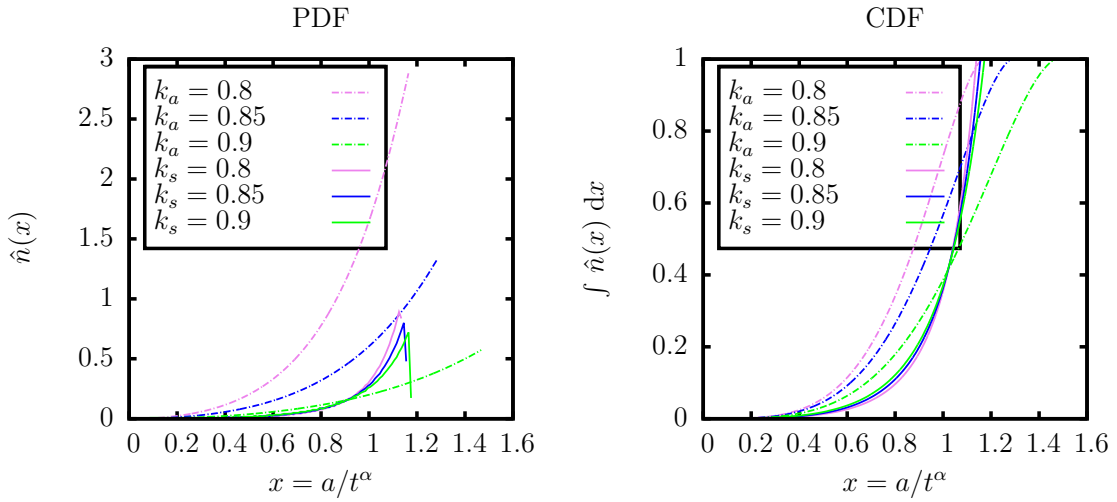

Figure 5.3.: Comparing the obtained distributions from section 2.3, we call the corresponding parameters k_a, and simulation, where k_s is the parameter.

We see a substantial difference in the distributions, so the ansatz does not represent the distribution in a convenient way. The next step will be to start with another ansatz $n(a,t)$ that depends on a polynomial of t and not just on $t^{-\beta}$.

A. Numerical Treatment

We assign an initial radius $a_i(0)$ to each droplet, $i = 0, \ldots, N_0 - 1$, such that the sequence $(a_n(0))_{n=0,\ldots,N_0-1}$ is strictly increasing. The differential equations we will apply do not change the order of the droplets. So the cumulative distribution $C(a)$ is readily obtained from the function $C(a_i) = i/N$. Thus, no sort algorithm is needed. The ODE (2.3) or (2.4) that describes the growth of droplets is solved by the Runge-Kutta method with a fixed step size $\Delta t = 10^{-3}$. Applied to the system of droplets the radius a_i of the ith droplet changes. If the droplet size falls below a predefined value $\rho_0 = 10^{-4}$ we take the droplet out of the system and decrease the number of droplets N by 1. This reflects the evaporation of small droplets due to their surface tension contribution. A finite value for ρ_0 is chosen to avoid encountering negative droplet radii. They occur since the step size is not small enough to get exactly the value zero for such a droplet. An adaptive Runge-Kutta method is not used as the step size will fall below the smallest resolvable value following exactly the final stages of droplet evaporation, and the smallest droplets are not of so much interest here.

At some point there will be just one big droplet that grew at the expense of the removed droplets if we continue this way. But the droplet size distribution of this single droplet is quite trivial, so we rather wish to keep the number of droplets above a chosen number $N_c = 1000$. Having reached N_c we double our system size to get again $N = 2000$ droplets. This is done by inserting droplets with the size of the arithmetic mean of every pair of consecutive droplets. This preserves the shape of the droplet size distribution and has only a small effect on the overall droplet volume per unit volume. It is important not to forget the average of the smallest and largest droplet that we insert such that the sequence $(a_n)_n$ stays strictly increasing. The variable V_{sys}, the volume of the system where we put the droplets in, is initialized with 1 and doubled every time the system size is doubled. We use it to rescale the total droplet volume to the original system size. We do not try to keep the total volume $V_{\text{tot}} = \sum_{i=1}^{N} a_i^3$ constant, so after doubling this term is slightly smaller.

For droplet sedimentation the probability of a droplet to die is compared to a random number generated by Mersenne-Twister and the droplet is removed from the system if the random number is smaller than the probability.

B. Excursion: Oscillatory Variation of the Ambient Temperature

In section 3.2 we considered a differential equation that describes systems with non-constant temperature. In order to describe clouds we are interested in how this equation can be adapted to even more general cases. When we look at clouds we see that apart from the non-constant temperature we have an oscillating temperature due to air parcels lifted up or descending with decreasing or increasing temperature, respectively. In convective clouds, a series of ascends and descends is experienced by air parcels driving rain formation. When air parcels rise and undergo an adiabatic expansion, T changes according to $\frac{p}{p_0} = \left(\frac{T}{T-\Delta T}\right)^{1-1/\gamma}$, p and p_0 being the different pressures and γ the ratio of specific heats [2]. So even in the absence of nucleation and droplet growth the temperature in a cloud depends on the height. To gain insight into these effects we study the effect of a slowly oscillating driving force. We remember that the parameter k controls whether the temperature increases or decreases in the system. So the intuitive way is to replace the previously used k by an oscillating expression also ranging around one, i.e. $k = 1 - k_0 \cos(\omega t)$, choosing

$$k_0 \in [10^{-5}, 0.9],\ \omega \in [0.0001, 100].$$

The system of differential equations that describes these systems is then

$$\dot{a}_i = \left(\frac{a_i}{\overline{a}} - 1 + k_0 \cos(\omega t)\right) \cdot \frac{1}{a_i^2} \tag{B.1}$$

Now we investigate the droplet volume fraction and $\overline{a}^3/t$ depending on k_0 and ω. Therefore, we calculate the average of $\sum_i a_i^3/V_{\text{sys}}$ in each period and pick the last period in the time interval $[0, 10^4]$. Since for too small ω the duration of an oscillation period T becomes very large compared to the integration time, using $T = 2\pi/\omega$, the crossover time is not reached for all considered k_0, ω, thus does not necessary lead to a reliable result. The same holds for the case that T is not much bigger than the

time step between the saved values, which is 0.1 here, because the number of values in one period is small and hence the average calculation has no effect. Thus, if p is the number of periods that are observed during the integration time 10^4, we exclude the values k_0 and ω that imply $p < 5$ or $p > 2 \cdot 10^4$, so we have at least five values to calculate the average.

Firstly, we are interested in the evolution of the droplet volume fraction $\sum_i a_i^3/V_{\text{sys}}$ depending on k_0 and ω. The average over the latest observed period is displayed in figure B.1, using above considerations.

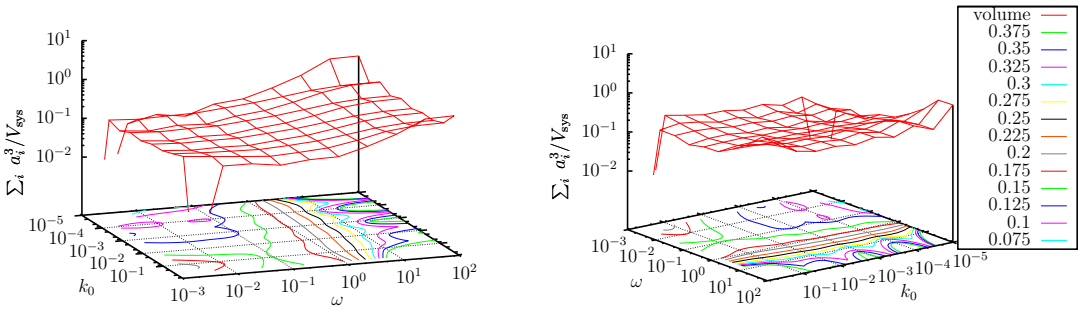

Figure B.1.: Volume depending on k_0 and ω in the last observed oscillation period. We observe that $V_{\text{tot}} \propto \omega^q, q > 0$, since the contour lines show in this area a constant volume for a fixed ω and arbitrary k_0, except for very small or very big values of ω. The distance between the straight lines is nearly the same, so the logarithmic scale suggests a powerlaw with $q = 1$.

Still, one can see that at the maximal and minimal values of the parameters the curve shape changes abruptly. So the requested p does not exclude enough critical cases. Due to the derivation (2.5a) we expect that $V_{\text{tot}} \propto t$, which implies $V_{\text{tot}} \propto \omega$ since we observe for increasing ω more oscillation periods in the system. A power law dependence is covered in the simulation for adequate p. We look closer at the

Secondly, similar to the previous cases, we explore the averaged asymptotic value of $\overline{a}^3/t$ in figure B.2.

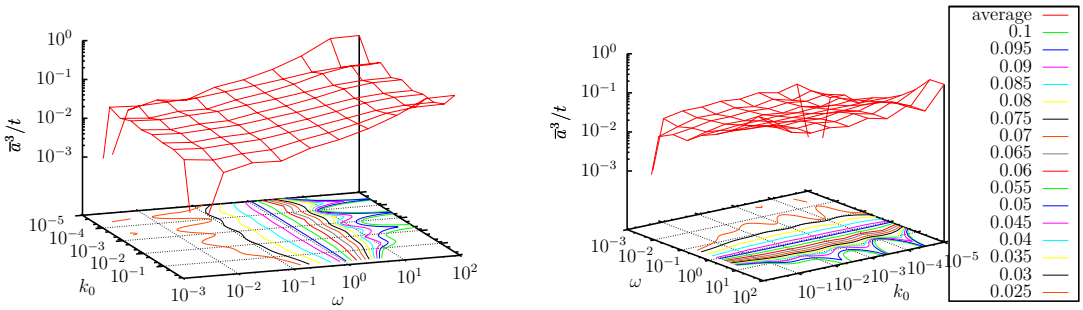

Figure B.2.: The asymptotic value $\overline{a}^3/t$ depending on the parameters k_0 and ω. For very small or very big ω there is a discrepancy in the curve shape. Apart from this, the asymptotic value $\overline{a}^3/t$ is constant for fixed ω. Furthermore, due to the logscale we can gather $\overline{a}^3/t \propto \omega^r, r > 0$ and since the distances between the straight lines are nearly the same it holds $r = 1$.

We also checked rectangular oscillations, substituting the cos with a function χ

$$\chi(x) = \begin{cases} 1, & x \in \left[-\frac{\pi}{2}, \frac{\pi}{2}\right] \\ -1 & x \in \left[\frac{\pi}{2}, \frac{3\pi}{2}\right] \end{cases} .$$

A difference in the results is not observed. This is due to the fact that these quantities change up to their average in one period, which is the same for both oscillating functions.

Bibliography

[1] M. P. Allen and D. J. Tildesley. *Computer Simulation of Liquids*. Oxford University Press, 1989.

[2] H.B. Callen. *Themodynamics*. Wiley, 1985.

[3] L. D. Landau and E. M. Lifshitz. *Lehrbuch der theoretischen Physik*, volume X. Physikalische Kinetik. Akademie, Berlin, 1983.

[4] T. Lapp, M. Rohloff, J. Vollmer, and B. Hof. Particle tracking for polydisperse sedimenting droplets in phase separation. *Experiments in Fluids*, 2011. submitted to Experiments in Fluids.

[5] I. M. Lifshitz and V. V. Slyozov. The kinetics of precipitation from supersaturated solid solutions. *J. Phys. Chem. Solids*, 19(1–2):35–50, 1961.

[6] H. R. Pruppacher and J. D. Klett. *Microphysics of Clouds and Precipitation*. Springer, 1996.

[7] M. Rohloff. *Measuring the Droplet-Size and Velocity Distributions in Binary Phase Separation*. 2011.

[8] R. A. Shaw. Particle-turbulence interactions in atmospheric clouds. *Annual Review Fluid Mechanics*, 35:183–227, January 2003. doi: 10.1146/annurev.fluid.35.101101.161125. cloud formation.

[9] R. A. Shaw and A. B. Kostinski. Fluctuations and Luck in Droplet Growth by Coalescence. *Bulletin of the American Meteorological Society*, 86:235–244, February 2005. doi: 10.1175/BAMS-86-2-235.

[10] J. Vollmer, G. K. Auernhammer, and D. Vollmer. Minimal model for phase separation under slow cooling. 98:115701, March 2007. doi: 10.1103/PhysRevLett.98.115701. URL `http://link.aps.org/abstract/PRL/v98/e115701`.

[11] G. Woan. *The Cambridge Handbook of Physics Formulas*. Cambridge University Press, 2000.

Acknowledgements

I would like to thank all those, who helped and supported me in creating this thesis.
First and foremost, I would like to thank my supervisor Jürgen Vollmer for his generosity, his patience and for introducing me to the vast landscape of scaling theory.
I also thank Prof. Rehren for his commitment as co-supervisor.
I wish to thank my parents for believing in me and for their enduring support.
For fruitful discussion, many thanks are due to Bernhard Altaner, Johannes Blaschke, Tobias Lapp, Jan-Hendrik Trösemeier and all other attendants of our PoSO group seminar.
Moreover, I would like to thank Daniel Herde, who sparked my interest in Python.
Last but not least, I wish to thank Alexander for proofreading, for his support and for encouraging me to finish this work.

Erklärung nach §13(8) der Prüfungsordnung für den Bachelor-Studiengang Physik und den Master-Studiengang Physik an der Universität Göttingen:

Hiermit erkläre ich, dass ich diese Abschlussarbeit selbständig verfasst habe, keine anderen als die angegebenen Quellen und Hilfsmittel benutzt habe und alle Stellen, die wörtlich oder sinngemäß aus veröffentlichten Schriften entnommen wurden, als solche kenntlich gemacht habe.
Darüberhinaus erkläre ich, dass diese Abschlussarbeit nicht, auch nicht auszugsweise, im Rahmen einer nichtbestandenen Prüfung an dieser oder einer anderen Hochschule eingereicht wurde.

Göttingen, den 4. Juli 2011

(Ariane Papke)